Downregulation of SNX5 By KLF9 Leads to Clear Cell Renal Cell Carcinoma Progression By Inducing CD44 Internalization and Suppressing Epithelial-to-Mesenchymal Transition

Qingqing Zhou
Shanghai Jiao Tong University School of Medicine Affiliated Renji Hospital
Jiajun Li
Shanghai Jiao Tong University School of Medicine Affiliated Renji Hospital
Chao Ge
Shanghai Jiao Tong University School of Medicine Affiliated Renji Hospital
Jinsi Chen
Shanghai Jiao Tong University School of Medicine Affiliated Renji Hospital
Wei Tian
Shanghai Jiao Tong University School of Medicine Affiliated Renji Hospital
Hua Tian (htian@shsci.org)
Shanghai Cancer Institute

Research

Keywords: SNX5, CD44, EMT, KLF9, progression, clear cell renal cell carcinoma

Posted Date: May 13th, 2021

DOI: https://doi.org/10.21203/rs.3.rs-500950/v1

Version of Record: A version of this preprint was published at Molecular Therapy - Oncolytics on December 1st, 2021. See the published version at https://doi.org/10.1016/j.omto.2021.12.002.

Abstract

Background: Aberrant expression of SNX5 can contribute to tumourigenesis, invasion, and metastasis of several human cancers. However, the clinicopathological and biological significance of SNX5 in clear cell renal cell carcinoma (ccRCC) remain unclear. The aim of this study was to examine the role of SNX5 in the progression of ccRCC.

Methods: Immunohistochemical (IHC), Western blot, qRT-PCR, western blot, flow cytometry and immunofluorescence were used to detect the expression of indicated molecules. The biological role of SNX5 in ccRCC cells was evaluated by CCK8, colony formation, transwell assay, subcutaneous tumor formation as well as veil tail injection. ChIP assay and luciferase reporter assay were used to determine the direct binding of KLF9 to the promoter of the SNX5 gene.

Results: SNX5 expression was downregulated in human ccRCC tissues. SNX5 expression was negatively correlated with tumor size, AJCC stage, tumor thrombus of inferior vena cava (IVC) and poor prognosis of ccRCC. Ectopic expression of SNX5 inhibited ccRCC cell proliferation and metastasis whereas knockdown of SNX5 increase these activities both in vitro and in vivo. Mechanistically, overexpression of SNX5 blocked internalization and intracellular trafficking of CD44 in ccRCC cells. Exogenous expression of CD44 partially rescued the inhibitory effects of SNX5 on the proliferation and invasion activity of ccRCC cells. Knockdown of SNX5 in ccRCC cells was associated with epithelial mesenchymal transition (EMT), including the down-regulation of E-cadherin, ZO-1 and Claudin-1 and the concomitant up-regulation of Snail and N-cadherin. In addition, SNX5 inhibited TGF-β-induced migration, invasion and EMT in ccRCC cells. Moreover, we observed a significant correlation between SNX5 expression and E-cadherin levels in ccRCC patients. In addition, KLF9 directly bound to the SNX5 promoter and increased SNX5 transcription. SNX5 expression was closely correlated with KLF9 expression in ccRCC. Moreover, we found that the combination of SNX5 and CD44 or E-cadherin or KLF9 was a more powerful predictor of poor prognosis than either parameter alone.

Conclusion: Collectively, our data reveal a mechanism that KLF9-mediated SNX5 expression was associated with poor prognosis via trafficking of CD44 and promoting EMT in ccRCC. SNX5 may be a potential prognostic biomarker and therapeutic target for patients with ccRCC.

Introduction

Kidney cancer is among the top ten malignant tumors, representing 4.1% of all new cancer cases, and it is estimated that 73820 people will be diagnosed in 2019 in the United States [1].Clear cell renal cell carcinoma (ccRCC) is the most common form of kidney cancer, accounting for up to 85% of cases [2]. In recent years, there has been further in-depth understanding of the underlying pathways driving ccRCC biology, resulting in notable improvements in diagnosis and therapeutics [3]. However, owing to recurrence and metastatic diseases, in additional to lacking of effective treatments, the prognosis of

ccRCC remains still poor [4].Therefore, it is urgent to elucidate the molecular mechanism of ccRCC and explore new therapeutic targets.

Sorting Nexin (SNXs) is a family that regulates the endocytosis of eukaryotic cells discovered in recent years [5].This family is a relatively conservative in the process of biological evolution, and its structure contains the Phoxhomology (PX) domain, which is tightly combined with phosphoinositol in the membrane structure [6]. As part of a retromer complex, SNXs play a critical part in transmembrane transport, protein sorting, intracellular signal transduction and organelle movement [7]. Therefore, SNXs family members are closely related to the occurrence and development of tumors.SNX16 expression was significantly upregulated in colorectal cancer (CRC) tissues. Upregulated SNX16 predicted poor survival of CRC patients [8]. SNX10 acts as a tumor suppressor which inhibits colorectal cancer initiation and progression [9].SNX1 expression is significantly downregulated in colon cancer [10]. Knockdown of SNX1 expression can significantly increase the phosphorylation level of EGFR and promote colon cancer cells proliferation [11].SNX6 predicts poor prognosis and contributes to the metastasis of pancreatic cancer cells via activating epithelial-mesenchymal transition (EMT) [12].SNX27 promotes breast cancer metastasis and the elevated expression of SNX27 could be related to the marginally shorter survival of the patients [13].Our previous research shows that SNX5 predicts poor prognosis and promotes hepatocellular carcinoma progression by modulating the EGFR-ERK1/2 signaling pathway [14]. However, the biological role and molecular mechanism of SNX5 in ccRCC remain unknown. In the present study, we analyzed the expression levels and clinical significance of SNX5 in ccRCC patients, and investigated the molecular mechanism underlying its role.

Materials And Methods

Cell lines

786-O, 769-P, Caki-1and ACHN were purchased from the Cell Bank of the Chinese Academy of Sciences (Shanghai, China). HEK-293T cell lines were purchased from the American Type Culture Collection (Manassas, VA, USA). 786-O, 769-P were cultured in RPMI 1640 medium, Caki-1 were cultured in McCoy's 5A medium, ACHN and HEK-293T were cultured in DMEM medium containing 10% fetal bovine serum (FBS), 100 U/ml penicillin and 100 U/ml streptomycin at 37 °C with 5% CO_2.

Immunohistochemistry (IHC)

This study was conducted in accordance with the International Ethical Guidelines for Health-related Research Involving Humans and was approved by the Research Ethics Committee of Renji Hospital. A total of 150 pathologically confirmed ccRCC and 30 adjacent normal kidney tissues were collected by Shanghai National Engineering Research Center from Taizhou Hospital from 2008 to 2015.

IHC assays were conducted as reported previously. Briefly, the sections were deparaffinized with xylene and rehydrated before being heated to just below boiling temperature in Tris/EDTA buffer pH 9.0 for 20 minutes in a microwave oven for antigen retrieval. The primary antibodies used for the IHC assay were

against SNX5. Scores of staining intensity were: 0, negative; 1, weak; 2, moderate; 3, strong. Scores of positively stained cell proportion were: 0, no positive; 1, <10%; 2, 10%–35%; 3, 35%–75%; 4, >75%.The results were scored 0 to 4 by two independent investigators. The individual scores for the staining intensity and percentage of positivity cells were then multiplied to calculate the immunoreactivity score for each sample. Samples having a final staining score of ≤4 were considered to exhibit low expression and those with a score of >4 were considered to be exhibit high expression.

Plasmids construction and lentivirus production

The plasmids coding sequences for human SNX5 and CD44 were constructed in our laboratory. The SNX5 lentiviral plasmid was supplied by GeneCopoeia (Guangzhou, China). psPAX2 and pMD2.G plasmids were purchased from Addgene (USA). According to manufacturer's protocol, 293T cells were transfected with a mixture of overexpressing or interfering plasmid, psPAX2 and pMD2.G plasmids for lentivirus packaging using Lipofectamine™ 2000 (Invitrogen, USA).The viruses were collected after harvesting 48-72h and added to ccRCC cells with 1×10^6 recombinant lentivirus-transducing units in the presence of 6 μg/ml polybrene (Sigma, USA).The target sequences are listed in Supplementary Table S1.

Quantitative real-time polymerase chain reaction (qRT-PCR)

Total RNA was retracted with TRIzol reagent (Invitrogen, USA) and was reverse-transcribed with a PrimeScript TM RT Reagent kit (TaKaRa, China).RT-qPCR was performed with an ABI Prism 7500 System (Applied Biosystems, USA) with SYBR Green Maste (Takara, China). All primer sequences are listed in Supplementary Table S2.

Western blot

Total proteins extracted from the cells were lysed with RIPA buffer (Thermo Scientific, USA) and separated on 8% - 12% SDS-PAGE gels, transferred onto polyvinylidene fluoride (PVDF) membranes (Millipore, USA), incubated with primary antibodies overnight at 4°C, probed with HRP-conjugated secondary antibodies, and visualized using enhanced chemiluminescence reagent (Pierce, USA) via a chemiluminescence analyzer (Bio-Rad, USA). Information on the antibodies is listed in Supplementary Table S3.

Cell proliferation and colony formation assays

Briefly, for CCK8 assay 600-800 cells/well were seeded in 96-well plates. After overnight, the CCK8 solution and the culture solution are mixed at a ratio of 1:9, the mixture is 100μL/well, incubated at 37°C 2 hours, the absorbance value is at A450nm. For colony formation assays, cells were seeded in each well of a 6-well plate and incubated at 37°C. After 1-2 weeks, discarded the culture medium and fixed it with formalin for 30 minutes. Added the Giemsa staining solution and placed it on a shaker overnight. Scanned and counted the number of clones using Image J software.

Transwell assay

Inoculated 4×10^4 cells in 200 μl of serum-free medium, put in the upper chamber of a transwell (8 μm pore size) or Matrigel coated transwell upper cavity. The lower chamber contains RPMI 1640medium with 10% fetal bovine serum as a chemotactic agent. After incubating for 6-8 hours at 37°C, took out the transwell and fixed it with formalin, stain with crystal violet for 10-15 minutes, used a cotton swab to gently wipe off the non-migrated or non-invaded cells from the upper chamber. And choosed five random fields of view to count under the microscope.

Flow cytometry analysis

To detect the population of E-cadherin$^+$ or the population of CD44$^+$, cells were plated in a 6-well plate and incubate at 37°C overnight, digested with trypsin the next day, washed the cells twice with PBS, added the corresponding antibodies and incubated on ice for 45 minutes, avoid light. Afterwards, the supernatant was discarded, and the cells were washed twice with PBS for flow cytometry analysis. The antibodies used are shown in Supplementary Table S3.

Immunofluorescence confocal imaging

The cells were inoculated on Lab-Tek laboratory slides one day in advance, and fixed with 4% paraformaldehyde at room temperature for 30 minutes the next day, washed three times with PBS; then 0.1% Triton X-100 was permeated for 5 minutes. Washed three times with PBS, added the primary antibody, 4 °C overnight, washed three times with PBS, incubated in Alexa Fluor 594-conjugated and Alexa Fluor 534-conjugated secondary antibodies and 4', 6-diamidino-2-phenylindole (DAPI) in blocking solution for 30 minutes at 37°C in a humidified chamber, washed three times and took pictures on Leica TCS SP8 confocal system (Leica, Microsystems). Information on the antibodies is listed in Supplementary Table S3.

Internalization and recycling assays

Internalization and recycling assays were conducted as reported previously [14].Firstly, Seeded cells in 6-cmdishes, the next day reached 80%-100%confluence. Secondly, placed the cells at 4°C and washed them twice with cold PBS. Thirdly, labelled the cell surface with 2 mL of 0.05 mg/mL cleavabe EZ-Link^{TM} sulfo-NHS-SS-biotin (biotin), 4°C, 30min. Fourth, Unlabeled biotin was washed three times in cold PBS containing 100 mM glycine. Fifth, added pre-warmed serum-free RPMI 1640 to the cells, and internalized the biotin-labeled surface protein at 37°C at the specified time point, transferring the cells to 4°C to stop internalization. Sixth, washed three times in pre-cooled stripping buffer (reduced 50 mM L-GSH, 75 mM NaCl, 75 mM NaOH, 1% bovine serum albumin (BSA) and 10 mM EDTA, pH 8.0), each time 10 minutes to remove surface biotin.

For recycling assays, the biotin-labeled surface protein was internalized at 37°C for 30 minutes. The surface biotin was removed as described above. After treatment with stripping buffer, the cells were washed once in cold medium. Added pre-warmed serum-free growth medium and incubated the cells at 37°C for the specified time point. Finally, incubated the cell lysate with streptavidin-coupled agarose

beads at 4°C for 2 hours. The agarose bead mixture was washed three times in RIPA buffer, and then the biotinylated protein was detected by Western blot analysis.

Luciferase assay

The SNX5 promoter (-1297 bp /40 relative to the transcription start site) was cloned into the luciferase reporter gene vector pGL3-Basic (Promega).. The fidelity of the constructs were confirmed by sequencing. The primer sequences are listed in Supplementary Table S2.

Cells were cotransfected with the corresponding reporter plasmid and the indicated plasmids in each experiment according to the standard protocol. The pRL-TK reporter construct was used as the internal control. Luciferase activity was detected using a Dual-Luciferase Report Assay (Promega) system in accordance with the manufacturer's instructions.[15].

In vivo growth and metastasis assays

Invivo growth, nude mice were injected with a total of 6× 10^6 cells suspended in 200μl of a mixture of serum-free RPMI 1640/Matrigel (1:1 volume) (BD Biosciences, MA) into the left axillary fossa. For metastasis assay, 2× 10^6 cellssuspended in 200μl ofserum-free RPMI 1640 injected into nude mice via tail vein injection. Eight weeks later, the mice were sacrificed, and the tumors and lung tissues were excised and fixed with 4% phosphate-buffered neutral formalin for at least 72 h. Metastatic tissues were analyzed by H&E staining. All of the experiments were approved by the Shanghai Medical Experimental Animal Care Commission.

Statistical analysis

Statistical analyses were performed using SPSS16.0 software. All data are presented as the mean ± SD. The correlation between SNX5 expression and E-cadherin was performed using Pearson's coefficient tests. Statistical comparisons of the data were performed using two-tailed Student's *t*-test or one-way ANOVA for multiple comparisons. Chi-square tests or fisher's exact tests were used to analyze the correlation between the expression of SNX5 and clinicopathological features. Overall survival curves were calculated using the Kaplan-Meier method and compared using the log-rank test. Univariate and multivariate analyses were performed using the Cox proportional hazard regression model in a stepwise manner. $p < 0.05$ was considered statistically significant.

Results

SNX5 is down-regulated and correlates with prognosis of ccRCC patients

To explore the role of SNX5 in ccRCC, we first detected the expression of SNX5 using data sets from TCGA (The Cancer Genome Atlas).The results showed that the expression of SNX5 was downregulated in

ccRCC tissues compared with noncancerous tissues (Fig. 1A). Furthermore, expression of SNX5 was downregulated in ccRCC based on the GSE15641 and GSE126964 datasets (Fig. 1B-1C). To investigate these findings further,we next analyzed SNX5 protein expression using immunohistochemistry and a tissue microarray of patient-derived ccRCC samples (*n* = 30) and matched normal kidney samples (*n* = 30).Of the 30 pairs, 24 (80%) had higher SNX5 protein expression in nontumor tissues than in tumor kidney tissues, 4 (13.3%) had similar expression, whereas only 2 (6.7%) had lower expression (Fig. 1D).In addition, expression of SNX5 was also down-regulated in ccRCC tumor tissue and noncancerous tissues using the Clinical Proteomic Tumor Analysis Consortium (CPTAC) datasets (Supplementary Fig. S1). Taken together, the results of these analyses show that SNX5 is downregulated in ccRCC.

We next detected the expression of SNX5 in 150 cases of ccRCC using IHC. According to the IHC results, the expression intensity of SNX5 protein was scored. A score of 0 to 4 was considered to represent low expression and a score of >4 was considered to represent high expression (Fig. 1E). Our results showed that expression of SNX5 was closely associated with tumor size, American Joint Committee on Cancer (AJCC) stage and *tumor thrombus of* inferior *vena cava (IVC)* (Table 1).Kaplan-Meier survival analysis revealed that lower levels of SNX5 were associated with a shorter overall survival (OS) time (*p* = 0.009; Fig. 1F). The same results were also found from the TCGA ccRCC cohort (*p* = 0.023; Fig. 1G). Moreover, univariate and multivariate COX regression analysis showed that a low level of SNX5 was associated with worse survival of ccRCC patients (Table 2). Therefore these findings indicate that SNX5 may serve as a valuable prognostic factor for ccRCC patients after surgery.

SNX5 inhibits the proliferation and tumourigenicity of ccRCC cells

Due to the fact that expression of SNX5 is associated with tumor size and *tumor thrombus* in ccRCC led us to rationalize that SNX5 might be important for ccRCC tumor growth and metastasis. To determine this possibility, 769-P, Caki-1 and 786-O cells were chosen for loss- or gain-of-function studies due to their high or low endogenous SNX5 levels (Supplementary Fig. S2).CCK8 and colony formation assays showed that the overexpression of SNX5 inhibited ccRCC cell proliferation and colony formation ability, while the knockdown of SNX5 significantly promoted cell proliferation and colony formation ability (Fig. 2A-2F). Next, we examined the effect of SNX5 on the tumourigenicity of ccRCC in vivo by using subcutaneous tumor model in nude mice. As shown in Fig. 2G, compared with the control group, 786-O overexpressing SNX5 inhibited tumor growth as determined by tumor volume and tumor weights. In contrast, tumors with shSNX5 exhibited larger volumes and higher weights than tumors with shNC in Caki-1 cells (Fig. 2H). Furthermore, expression of Ki-67 and PCNA was significantly reduced in ccRCC cells with SNX5 overexpression and enhanced in ccRCC cells with SNX5 knockdown (Fig. 2I-2J). Taken together, these results provide strong evidence that SNX5 inhibits the tumorigenic ability of ccRCC cells.

SNX5 inhibits invasion and metastasisof ccRCC in vitro and in vivo

To explore whether SNX5 is necessary for ccRCC metastasis, we first analyzed the effects of *SNX5*overexpression or knockdown on ccRCC cell migration and invasion. Our results showed that overexpression of SNX5 inhibited ccRCC migration and invasion, while knockdown of SNX5 resulted in

significant increase in ccRCC cells migration and invasion (Fig. 3A-3B). In addition, we found that overexpression of SNX5 decreased MMP9 expression in ccRCC cells, whereas the knockdown of SNX5 increased MMP9 expression in ccRCC cells (Fig.3C-3D).

To determine whether *SNX5* expression plays a role in ccRCC metastasis in vivo, we injected ccRCC cells expressing Vector or *SNX5* into the tail veins of mice to mimic lung metastasis. Histological examination of lung tissues indicated that SNX5 overexpression tumor-bearing mice had significantly lower numbers of lung metastatic nodules than the control group (Fig. 3E). Taken together, our findings demonstrate that SNX5 play an important role in the metastasis of ccRCC cells.

SNX5 negatively regulated epithelial to mesenchymal transition (EMT) in ccRCC cells

Epithelial-to-mesenchymal transition (*EMT*) is a key process by which cancer cells *acquire invasive and metastatic properties* [16].Our results demonstrated that SNX5 overexpression in 786-O and 769-P cells resulted in a morphological change in epithelial mesenchymal transition in ccRCC cells, from fiber to round shape, suggesting the inhibition of EMT transition (Fig. 4A). Then, we detected EMT markers in SNX5-overexpressing and SNX5 knockdown ccRCC cells. The results showed that epithelial markers E-cadherin, ZO-1 and Claudin-1 were increased in SNX5 overexpression 786-O and 769-P cells, whereas mesenchymal markers N-cadherin and transcription factors Snail were decreased. On the contrary, knockdown of SNX5 in 769-P and Caki-1 cells decreased the expression of E-cadherin, ZO-1 and Claudin-1, and was accompanied by increased the expression of N-cadherin and snail (Fig. 4B-4C).And, that is the same as the result of western blot on tumor tissues overexpressing and knockdown SNX5 (Fig. 4D-4E). Moreover, we used immunofluorescence to detect the expression levels of E-cadherin and N-cadherin in 769-P cells with stable overexpression of SNX5, the results were consistent with the findings obtained by Western blot (Fig. 4F).

We also detected the cell surface expression of E-cadherin in the SNX5-overexpressing and SNX5 knockdown ccRCC cells by flowcytometry. The results showed that SNX5 overexpression increased the expression of E-cadherin compared to the control group in 769-P cells. Conversely, knockdown of SNX5 significantly decreased the expression of E-cadherinin 769-P cells (Fig. 4G). Collectively, these results revealed that SNX5 negatively regulates EMT in ccRCC cells.

To further explore potential clinical applications, we next evaluated the expression of E-cadherin in ccRCC using data sets from TCGA. The results showed that expression of E-cadherin was downregualted in ccRCC tumor tissues compared with normal tissues (Supplementary Fig. S3A). In addition, E-cadherin protein expression was also down-regulated in ccRCC tumor tissue and noncancerous tissues using CPTAC datasets (Supplementary Fig. S3B). Then, we analyzed the relationship between SNX5 and E-cadherin using data sets from TCGA data. The results showed that there was a positive correlation between the expression of SNX5 and E-cadherin in ccRCC tissue (Supplementary Fig. S3C). Furthermore, Kaplan-Meier survival analysis revealed that lower levels of E-cadherin were associated with a shorter overall survival (OS) time based on TCGA (p = 0.000; Supplementary Fig. S3D). Moreover, the patients

with low expression of SNX5 and E-cadherin displayed a worse prognosis than the high SNX5 and E-cadherin groups based on TCGA (Fig. 4H).

TGF-β-induced EMT was partially reversed by SNX5 overexpression in ccRCC cells

Transforming growth factor β (TGF-β) is a secreted cytokine and may function as a tumor promoter by facilitating cancer cells to undergo EMT [17].Therefore, we investigated whether the SNX5 affects TGF-β-induced EMT in ccRCC cells. Our results showed that morphologically, overexpression of SNX5 partially inhibited TGF-β-induced EMT (Fig. 5A). Furthermore, elevated N-cadherin and Snail expression and reduced E-cadherin, ZO-1 and Claudin-1 expression in response to SNX5 overexpressing were alleviated by TGF-β treatment (Fig.5B). In addition, we used immunofluorescence to detect the expression levels of E-cadherin and N-cadherin in SNX5 overexpressing 769-P cells-treated with TGF-β. The results were consistent with the findings obtained by Western blot (Fig. 5C). Transwell assays showed that overexpression of SNX5 partly reversed the effect of TGF-β on promoting ccRCC cells migration and invasion (Fig. 5D). Thus, these data support the view that SNX5 negatively regulates EMT in ccRCC cells.

SNX5 inhibited ccRCC cell proliferation, migration and invasion by inducing CD44 internalization

Cancer cells that undergo an EMT acquire cancer stem cell-like properties and show an increase in CD44 expression [18].Therefore, we determined the effects of overexpression or knockdown of SNX5 on the marker of potential cancer stem cell (CSC). Our results showed that overexpression of SNX5 inhibited CD44 and Oct4 mRNA and protein expressionin 786-O and 769-P cells. Knockdown of SNX5 increased CD44 and Oct4 mRNA and protein expression in 769-P and Caki-1 cells (Fig. 6A-6D). And, that is the same as the result of western blot on tumor tissues overexpressing and knockdown SNX5 (Fig. 6E-6F).

In addition, our results showed that SNX5 overexpression decreased the cell surface expression of CD44 compared to the control group in 769-P cells, whereas knockdown of SNX5 significantly increased the cell surface expression of CD44 in 769-P cells (Fig.7A). Furthermore, confocal colocalization analysis also revealed that SNX5 overexpression had lower expression of CD44 in 786-O and 769-P cells (Fig. 7B). IHC demonstrated that CD44 was down regulated in murine xenografts from SNX5-overexpressing 786-O cells (Fig. 7C).

Considering SNX-mediated endosomal transport, we investigated whether the overexpression of SNX5 affects the internalization and recycling of CD44 in ccRCC cells. Our results showed that SNX5 overexpression caused a significant increase in CD44 internalization and affected its recycling to the cell surface (Fig. 7D-7F).

Next, we investigated whether the SNX5 inhibited ccRCC cell proliferation, migration and invasion through regulation of CD44.To confirm the role of CD44 in SNX5-inhibted cell proliferation, migration and invasion, we constructed CD44 expression vector to rescue its expression in SNX5 overexpression ccRCC cells. The results showed that the SNX5 overexpression inhibited cell proliferation, migration and invasion

was partially reversed by the overexpression of CD44 (Fig. 8A-8D).Therefore, all results show that SNX5 inhibited ccRCC cell proliferation, migration and invasion by regulation of CD44.

To further explore potential clinical applications, we next evaluated the expression of CD44 in ccRCC using data sets from TCGA. The results showed that expression of CD44 was upregualted in ccRCC tumor tissues compared with normal tissues (Supplementary Fig. S4A). In addition, CD44 protein expression was also upregulated in ccRCC tumor tissue and noncancerous tissues using CPTAC datasets(Supplementary Fig. S4B).Furthermore, Kaplan-Meier survival analysis revealed that high levels of CD44 were associated with a shorter overall survival (OS) time based on TCGA (p = 0.005. (Fig. 8E). In addition, the patients with low expression of SNX5 and high expression of CD44 played a worse prognosis than the high SNX5 and low CD44 groups according to TCGA, indicating that the combination of SNX5 and CD44 has better prognostic value than SNX5 or CD44 alone (Fig. 8F).

SNX5 is upregulated by KLF9 in ccRCC cells

Our analyses of previously published data from ccRCC samples revealed decreased *SNX5* at the mRNA level, leading us to hypothesize that the reduced expression was the result of altered transcriptional regulation. In order to identify potential transcriptional regulators of SNX5, we performed a reporter assay to identify the regulatory elements that control SNX5 transcription. We analyzed the SNX5 promoter via websites that predicted transcription factor binding sites (JASPAR database). Krüppel-like factor 9 (KLF9) transcription factor binding sites were observed in the promoter of SNX5 (Fig. 9A-9B). KLF9 generally function as transcriptional repressors [19]. Luciferase assay showed that knockdown of KLF9 inhibited the activity of SNX5 (Fig. 9C). In addition, knockdown of KLF9 inhibited the expression of SNX5 in ccRCC cells (Fig. 9D-9E). The binding of KLF9 to the promoter of SNX5 was further confirmed by ChIP assay (Fig. 9F). Furthermore, we found that there a significant positive correlation between the expression of KLF9 and SNX5 in ccRCC tissue (Fig. 9G, r=0.36, P<0.01). Therefore, all results suggested that KLF9 binds to the SNX5 promoter and increases its expression in ccRCC cells.

Low expression of SNX5 and KLF9 in ccRCC predicts a poor prognosis

To further explore potential clinical applications of the experimental data, we next assessed the expression of KLF9 in ccRCC based on the TCGA. We found that the expression of KLF9 was downregulated in the ccRCC tissues compared with noncancerous tissues (Fig. 9H). Analysis of the GES15641 cohort showed that the KLF9 mRNA level was downregulated in the ccRCC tissues compared with noncancerous tissues (Fig. 9I). Furthermore, the expression of KLF9 was negative associated with tumor stage, nodal metastasis and overall survival and disease free survival (Fig. 9J-9L).

Based on the expression of SNX5 and KLF9, ccRCC patients were classified into the following four groups: low SNX5 and low KLF9 group (n=154), low SNX5 and high KLF9 group (n=107), high SNX5 and low KLF9 group (n=118), high SNX5 and high KLF9 group (n=149). The patients with low expression of SNX5 and KLF9 displayed a worse prognosis than the low SNX5 or KLF9 alone, indicating that the combination of SNX5 and KLF9 has better prognostic value than SNX5 or KLF9 alone (Fig. 9M).

Discussion

In the present study, we found that expression of SNX5 is downregulated and associated with a worse prognosis in ccRCC patients. We found that SNX5 is an inhibitor of proliferation and metastasis in ccRCC cells. Mechanistically, SNX5 facilitates the internalization and inhibits the recycling of CD44 in ccRCC cells, thereby inhibiting EMT of ccRCC cells and exerting a tumor suppressor function.

As a member of the SNX family, SNX5 is involved in endocytosis and internalization of membrane proteins and lipids [20, 21]. Endocytosis is an essential component of cell motility. Therefore, endocytosis can influence the transformed cell behavior, including proliferation and metastasis [22, 23].However, role of SNX5 is different in various tumors. Previous studies showed that loss of SNX5 stabilizes internalized growth factor receptors to promote thyroid cancer progression [24]. However, SNX5 decreases the FBW7-mediated oncoproteins degradation to promote head and neck squamous cell carcinoma (HNSCC) progression [25]. Our previous studies showed that expression of SNX5 was upregulated and related with poor prognosis in HCC [14]. Therefore, SNX5 plays different roles in different types of human tumors. In this study, we found that expression of SNX5 was downregualted in ccRCC. The expression of SNX5 was closely associated with tumor size, AJCC stage tumor thrombus of inferior vena cava (IVC) and prognosis. Moreover, univariate and multivariate COX regression analysis showed that a low level of SNX5 was associated with worse survival of ccRCC patients. Therefore these findings indicate that SNX5 may serve as a valuable prognostic factor for ccRCC patients after surgery.

CD44, a non-kinase transmembrane glycoprotein, is widely expressed on cell membrane implicated in many physiological and pathological processes, which include development, inflammation, immune responses, wound healing and cancer progression [26, 27]. CD44 overexpression or alternative splicing was described for various types of cancers including ccRCC and associated with invasion, metastasis and resistance to chemotherapeutic drugs [28-30].CD44 is a known cargo of clathrin-independent endocytosis [31]. Acylation of CD44 is a critical driving force to CD44 association with lipid rafts, which is essential for the rates of hyaluronan endocytosis and CD44 turnover from cell surface [32].Yu,K.S et al show that receptor-meditated endocytosis by hyaluronic acid for targeting of CD44-overexpressing cancer cells has promising therapeutic prospects [33]. A large endocytic receptor LRP-1mediated internalization of CD44, which plays an important role in the adhesive properties of tumor cells [34]. Others present that chondrocytes regulate the internalization of CD44, and CD44 turnover is modulatedby occupancy with hyaluronan [35]. Here, we demonstrate that overexpression of SNX5 decreased the cell surface expression of CD44 and accelerated internalization of CD44 into the cytoplasm in ccRCC cells. Furthermore, overexpression of CD44 rescued the effects of overexpression of SNX5 on ccRCC cell proliferation and invasion. In addition, the patients with low expression of SNX5 and high expression of CD44 played a worse prognosis than the high SNX5 and low CD44 groups according to TCGA, indicating that the combination of SNX5 andCD44has better prognostic value than SNX5 or CD44 alone. Therefore, together our data suggest that downregulated SNX5 facilitated the localization of CD44 to the cell surface by recycling which is an important mechanism to promote ccRCC cell invasion and metastasis.

By regulating multiple important cellular signaling pathways including β-catenin, TGF-β, etc, CD44 is known to promote tumorigenesis and EMT [36-38]. Upregulation of CD44 facilitates EMT-phenotypic change at acquisition of resistance to EGFR kinase inhibitors in lung cancer [39].Our data demonstrate that downregulation of SNX5 decreased the expression of E-cadherin, ZO-1, Claudin-1, and was accompanied by increased the expression of N -cadherin and snail. Furthermore, knockdown of SNX5 promoted the expression of MMP9 in ccRCC cells. Therefore, the knockdown of SNX5 induces an EMT-like phenotypic transition and promotes metastasis in ccRCC. Furthermore, we found that overexpressed SNX5 inhibited TGF-β-induced EMT in ccRCC cells. TGF-β-induced cell migration and invasion was partially reversed by overexpression of SNX5, suggesting that TGF-β may contribute to these processes downstream of SNX5.

Based on the database analyses and our experiments, we find that KLF9 binds to the SNX5 promoter and increases its expression in ccRCC cells. KLF9 is a zinc finger-containing transcription factor that belongs to the KLF family, and is expressed in various human tissues. KLF proteins have important roles in the regulation of a wide variety of biological processes as well as human diseases, such as cancer [40]. KLF9 acts as a tumor suppressor which has been reported to suppress cell proliferation, migration, invasion [41-43]. Previous study also shows that KLF9 is downregulated and negatively associated with poor prognosis in human ccRCC [44]. In this study, we find that low expression of KLF9 is one of the reasons for the down-regulation of SNX5 in ccRCC. Furthermore, we find that combination of SNX5 and KLF9has better prognostic value for ccRCC patients. Therefore, downregulated SNX5 by the loss of KLF9 facilitates ccRCC proliferation and metastasis.

Conclusion

Our study shows that SNX5 is a tumor suppressor in ccRCC. Mechanistically, knockdown of SNX5 triggers CD44 internalization and recycling, resulting in increased cell surface CD44 expression and promoting cell proliferation and metastasis. Furthermore, expression of SNX5 is regulated by KLF9 in ccRCC cells. The combination of low SNX5, high CD44 and low KLF9 expression may serve as a predictor of poor prognosis in patients with ccRCC (Fig. 10). These findings shed new insights into the pathogenesis of ccRCC and may lead to the development of novel targeted therapies.

Abbreviations

SNXs: Sorting Nexin; CCRCC: kidney renal cell carcinoma; TCGA:T he Cancer Genome Atlas; GEO: Gene Expression Omnibus; qRT-PCR: Quantitative real-time RT-PCR;CCK8: Cell Counting Kit-8; PVDF: polyvinylidenefluoride; IHC: immunohistochemistry; TGF-β:transforming growth factor-β; EMT: epithelial-mesenchymaltransition; OS: overall survival; CSCs: cancer stem cells;

Declarations

Ethics approval and consent to participate

This study was conducted in accordance with the International Ethical Guidelines for Health-related Research Involving Humans and was approved by the Research Ethics Committee of Renji Hospital.

Consent for publication

Not applicable.

Availability of data and materials

All data generated or analyzed during this study are available from the corresponding author upon reasonable request.

Competing Interests

The authors declare that they have no conflict of interest.

Funding: This work was supported by grants from the National Natural Science Foundation of China (81972581), Natural Science Foundation of Shanghai (19ZR1452800), Shanghai Sailing Program (21YF1445400) and Foundation of Shanghai Municipal Health Commission (201940429).

Author Contributions

HT designed and performed experiments, analyzed data. QQZ, JJL, CG, JSC, and WT performed experiments. HT designed and supervised research and wrote the manuscript.

Acknowledgements

The RNA expression and ccRCC patient clinical information were obtained from the TCGA and GEO Research Network.

References

1. Siegel RL, Miller KD, Jemal A. Cancer statistics. 2019. CA: A Cancer Journal for Clinicians. 2019, 69(1):7–34.
2. Klatte T, Pantuck AJ, Kleid MD, Belldegrun AS. Understanding the natural biology of kidney cancer: implications for targeted cancer therapy. Rev Urol. 2007;9(2):47–56.
3. Pantuck AJ, Zeng G, Belldegrun AS, Figlin RA. Pathobiology, prognosis, and targeted therapy for renal cell carcinoma: exploiting the hypoxia-induced pathway. Clinical cancer research: an official journal of the American Association for Cancer Research. 2003;9(13):4641–52.
4. Ljungberg B. The role of metastasectomy in renal cell carcinoma in the era of targeted therapy. Curr Urol Rep. 2013;14(1):19–25.
5. Mayor S, Pagano RE. Pathways of clathrin-independent endocytosis. Nat Rev Mol Cell Biol. 2007;8(8):603–12.

6. Heucken N, Ivanov R. The retromer, sorting nexins and the plant endomembrane protein trafficking. J Cell Sci. 2018, 131(2).
7. Cullen PJ, Korswagen HC. Sorting nexins provide diversity for retromer-dependent trafficking events. Nat Cell Biol. 2011;14(1):29–37.
8. Shen Z, Li Y, Fang Y, Lin M, Feng X, Li Z, et al. SNX16 activates c-Myc signaling by inhibiting ubiquitin-mediated proteasomal degradation of eEF1A2 in colorectal cancer development. Mol Oncol. 2020;14(2):387–406.
9. Zhang S, Yang Z, Bao W, Liu L, You Y, Wang X, et al. SNX10 (sorting nexin 10) inhibits colorectal cancer initiation and progression by controlling autophagic degradation of SRC. Autophagy. 2020;16(4):735–49.
10. Nguyen LN, Holdren MS, Nguyen AP, Furuya MH, Bianchini M, Levy E, et al. Sorting nexin 1 down-regulation promotes colon tumorigenesis. Clin Cancer Res. 2006;12(23):6952–9.
11. Huang Z, Huang S, Wang Q, Liang L, Ni S, Wang L, et al. MicroRNA-95 promotes cell proliferation and targets sorting Nexin 1 in human colorectal carcinoma. Cancer Res. 2011;71(7):2582–9.
12. Hu P, Liang Y, Hu Q, Wang H, Cai Z, He J, et al. SNX6 predicts poor prognosis and contributes to the metastasis of pancreatic cancer cells via activating epithelial-mesenchymal transition. Acta Biochim Biophys Sin (Shanghai). 2018;50(11):1075–84.
13. Sharma P, Parveen S, Shah LV, Mukherjee M, Kalaidzidis Y, Kozielski AJ, et al. SNX27-retromer assembly recycles MT1-MMP to invadopodia and promotes breast cancer metastasis. J Cell Biol. 2020, 219(1).
14. Zhou Q, Huang T, Jiang Z, Ge C, Chen X, Zhang L, et al. Upregulation of SNX5 predicts poor prognosis and promotes hepatocellular carcinoma progression by modulating the EGFR-ERK1/2 signaling pathway. Oncogene. 2020;39(10):2140–55.
15. Zhou Q, Tian W, Jiang Z, Huang T, Ge C, Liu T, et al. A positive feedback loop of AKR1C3-mediated activation of NF-κB and STAT3 facilitates proliferation and metastasis in hepatocellular carcinoma. Cancer Res. 2020.
16. Thiery JP, Acloque H, Huang RY, Nieto MA. Epithelial-mesenchymal transitions in development and disease. Cell. 2009;139(5):871–90.
17. Hao Y, Baker D, Ten Dijke P. TGF-β-Mediated Epithelial-Mesenchymal Transition and Cancer Metastasis. Int J Mol Sci. 2019, 20(11).
18. Mani SA, Guo W, Liao MJ, Eaton EN, Ayyanan A, Zhou AY, et al. The epithelial-mesenchymal transition generates cells with properties of stem cells. Cell. 2008;133(4):704–15.
19. Knoedler JR, Subramani A, Denver RJ. The Krüppel-like factor 9 cistrome in mouse hippocampal neurons reveals predominant transcriptional repression via proximal promoter binding. BMC Genomics. 2017;18(1):299.
20. Simonetti B, Paul B, Chaudhari K, Weeratunga S, Steinberg F, Gorla M, et al. Molecular identification of a BAR domain-containing coat complex for endosomal recycling of transmembrane proteins. Nat Cell Biol. 2019;21(10):1219–33.

21. Merino-Trigo A, Kerr MC, Houghton F, Lindberg A, Mitchell C, Teasdale RD, et al. Sorting nexin 5 is localized to a subdomain of the early endosomes and is recruited to the plasma membrane following EGF stimulation. J Cell Sci. 2004;117(Pt 26):6413–24.
22. Poudel KR, Roh-Johnson M, Su A, Ho T, Mathsyaraja H, Anderson S, et al. Competition between TIAM1 and Membranes Balances Endophilin A3 Activity in Cancer Metastasis. Dev Cell. 2018;45(6):738–52.e736.
23. Chung BM, Tom E, Zutshi N, Bielecki TA, Band V, Band H. Nexus of signaling and endocytosis in oncogenesis driven by non-small cell lung cancer-associated epidermal growth factor receptor mutants. World J Clin Oncol. 2014;5(5):806–23.
24. Jitsukawa S, Kamekura R, Kawata K, Ito F, Sato A, Matsumiya H, et al. Loss of sorting nexin 5 stabilizes internalized growth factor receptors to promote thyroid cancer progression. J Pathol. 2017;243(3):342–53.
25. Cai J, Sun M, Hu B, Windle B, Ge X, Li G, et al. Sorting Nexin 5 Controls Head and Neck Squamous Cell Carcinoma Progression by Modulating FBW7. J Cancer. 2019;10(13):2942–52.
26. Orian-Rousseau V, Ponta H. Perspectives of CD44 targeting therapies. Arch Toxicol. 2015;89(1):3–14.
27. Pandey S, Mahtab A, Rai N, Rawat P, Ahmad FJ, Talegaonkar S. Emerging Role of CD44 Receptor as a Potential Target in Disease Diagnosis: A Patent Review. Recent Pat Inflamm Allergy Drug Discov. 2017;11(2):77–91.
28. Li X, Ma X, Chen L, Gu L, Zhang Y, Zhang F, et al. Prognostic value of CD44 expression in renal cell carcinoma: a systematic review and meta-analysis. Sci Rep. 2015;5:13157.
29. Wang A, Chen M, Wang H, Huang J, Bao Y, Gan X, et al. Cell Adhesion-Related Molecules Play a Key Role in Renal Cancer Progression by Multinetwork Analysis. Biomed Res Int. 2019, 2019:2325765.
30. Yin T, Wang G, He S, Liu Q, Sun J, Wang Y. Human cancer cells with stem cell-like phenotype exhibit enhanced sensitivity to the cytotoxicity of IL-2 and IL-15 activated natural killer cells. Cell Immunol. 2016;300:41–5.
31. Eyster CA, Higginson JD, Huebner R, Porat-Shliom N, Weigert R, Wu WW, et al. Discovery of new cargo proteins that enter cells through clathrin-independent endocytosis. Traffic. 2009;10(5):590–9.
32. Thankamony SP, Knudson W. Acylation of CD44 and its association with lipid rafts are required for receptor and hyaluronan endocytosis. J Biol Chem. 2006;281(45):34601–9.
33. Yu KS, Lin MM, Lee HJ, Tae KS, Kang BS, Lee JH, et al. Receptor-Meditated Endocytosis by Hyaluronic Acid@Superparamagnetic Nanovetor for Targeting of CD44-Overexpressing Tumor Cells. Nanomaterials (Basel). 2016, 6(8).
34. Perrot G, Langlois B, Devy J, Jeanne A, Verzeaux L, Almagro S, et al. LRP-1–CD44, a new cell surface complex regulating tumor cell adhesion. Mol Cell Biol. 2012;32(16):3293–307.
35. Aguiar DJ, Knudson W, Knudson CB. Internalization of the hyaluronan receptor CD44 by chondrocytes. Exp Cell Res. 1999;252(2):292–302.

36. Chang G, Zhang H, Wang J, Zhang Y, Xu H, Wang C, et al. CD44 targets Wnt/β-catenin pathway to mediate the proliferation of K562 cells. Cancer Cell Int. 2013;13(1):117.
37. Ouhtit A, Madani S, Gupta I, Shanmuganathan S, Abdraboh ME, Al-Riyami H, et al. TGF-β2: A Novel Target of CD44-Promoted Breast Cancer Invasion. J Cancer. 2013;4(7):566–72.
38. Janda E, Lehmann K, Killisch I, Jechlinger M, Herzig M, Downward J, et al. Ras and TGF[beta] cooperatively regulate epithelial cell plasticity and metastasis: dissection of Ras signaling pathways. J Cell Biol. 2002;156(2):299–313.
39. Suda K, Murakami I, Yu H, Kim J, Tan AC, Mizuuchi H, et al. CD44 Facilitates Epithelial-to-Mesenchymal Transition Phenotypic Change at Acquisition of Resistance to EGFR Kinase Inhibitors in Lung Cancer. Mol Cancer Ther. 2018;17(10):2257–65.
40. Bialkowska AB, Yang VW, Mallipattu SK. Krüppel-like factors in mammalian stem cells and development. Development. 2017;144(5):737–54.
41. Li Y, Sun Q, Jiang M, Li S, Zhang J, Xu Z, et al. KLF9 suppresses gastric cancer cell invasion and metastasis through transcriptional inhibition of MMP28. Faseb j. 2019;33(7):7915–28.
42. Bagati A, Moparthy S, Fink EE, Bianchi-Smiraglia A, Yun DH, Kolesnikova M, et al. KLF9-dependent ROS regulate melanoma progression in stage-specific manner. Oncogene. 2019;38(19):3585–97.
43. Brown AR, Simmen RC, Raj VR, Van TT, MacLeod SL, Simmen FA. Krüppel-like factor 9 (KLF9) prevents colorectal cancer through inhibition of interferon-related signaling. Carcinogenesis. 2015;36(9):946–55.
44. Huang C, Li J, Zhang X, Xiong T, Ye J, Yu J, et al. The miR-140-5p/KLF9/KCNQ1 axis promotes the progression of renal cell carcinoma. Faseb j. 2020;34(8):10623–39.

Figures

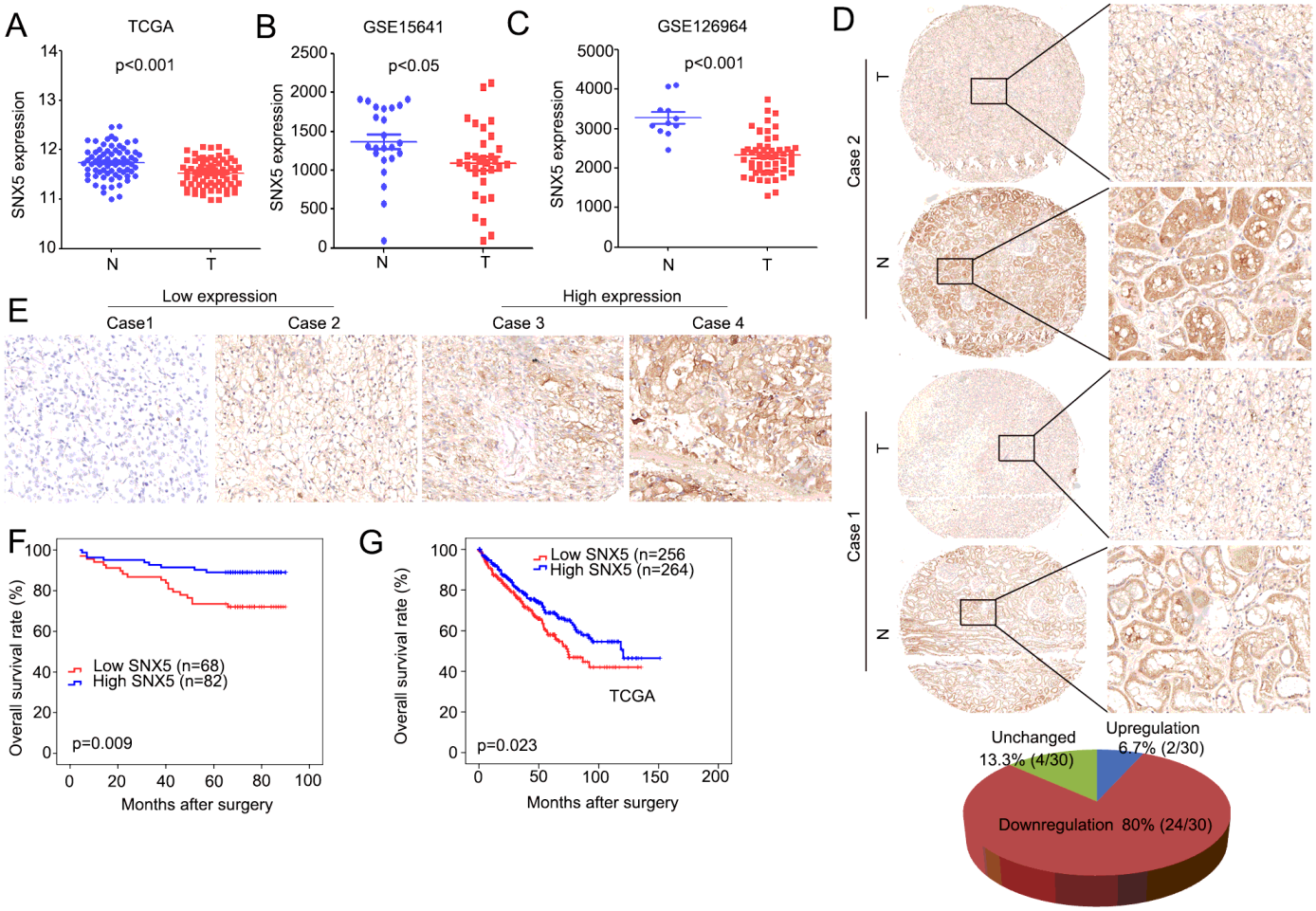

Figure 1

SNX5 is downregulated and is associated with poor prognosis in ccRCC patients. (A) The expression of SNX5 in ccRCC tissues compared with adjacent normal tissues was analyzed using data sets from TCGA. (B) The expression of SNX5 in ccRCC tissues compared with adjacent normal tissues was analyzed using data sets from GSE15641. (C)The expression of SNX5 in ccRCC tissues compared with adjacent normal tissues was analyzed using data sets from GSE126964. (D) Representative IHC images showing the expression of SNX5 in ccRCC tissues and adjacent normal tissues. (E) The expression of SNX5 in ccRCC tissues was cored, and representative IHC images were shown. (F) Kaplan-Meier analysis of overall survival (OS) according to SNX5 expression in 150 ccRCC patients. (G) Patients with low expression levels of SNX5 had shorter overall survival than patients with high expression levels as determined using data sets from TCGA.*P< 0.05; **P< 0.01.

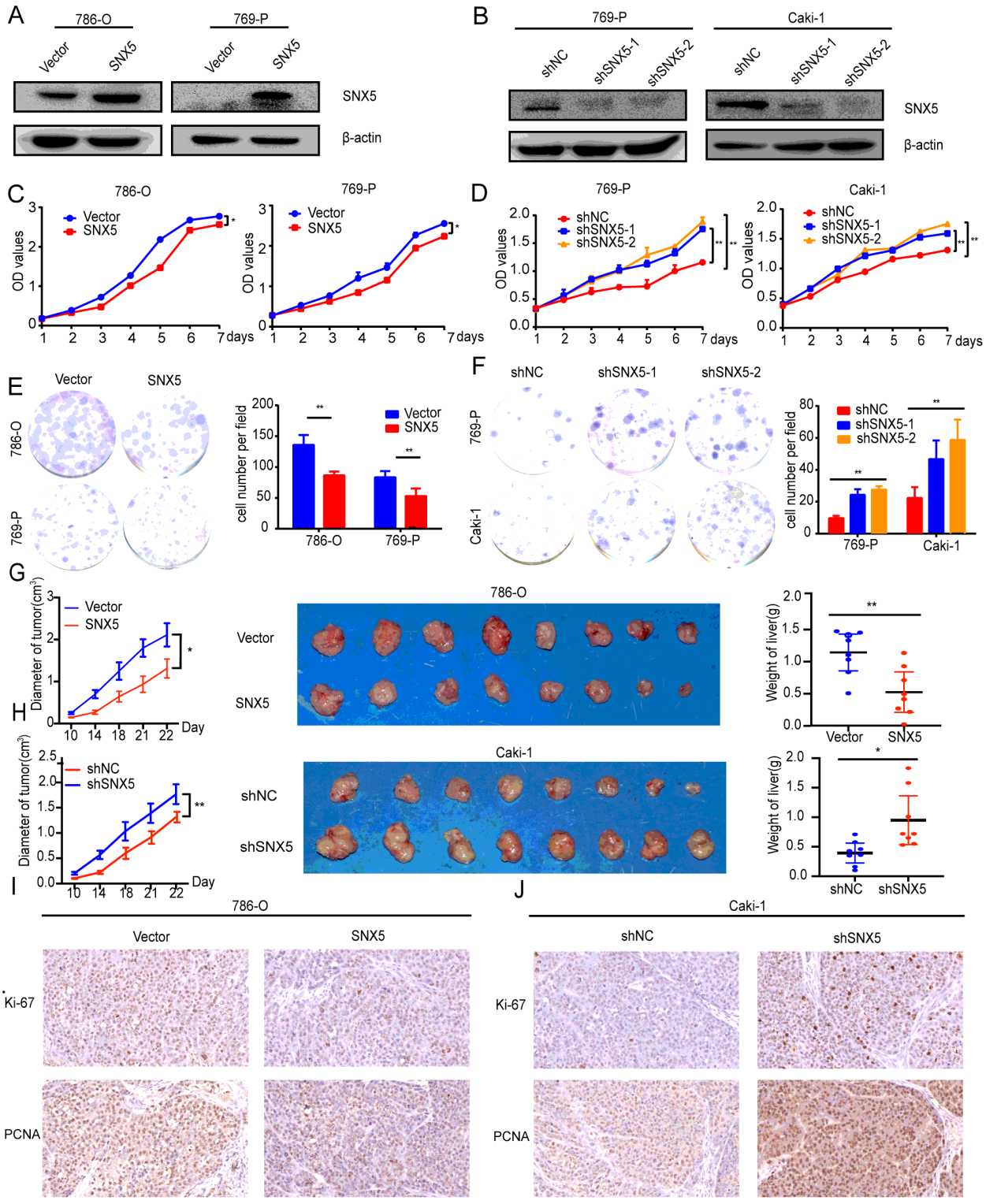

Figure 2

SNX5 inhibits ccRCC cell proliferation. (A) Western blot revealed that SNX5 was efficiently overexpressed in 786-O and 769-P cells. (B)Western blot revealed that SNX5 was efficiently knocked down in 769-P and Caki-1 cells.(C) CCK8 assay demonstrated that the overexpression of SNX5 inhibited CCRCC cells proliferation. (D) CCK8 assay demonstrated that knockdown of SNX5 promoted ccRCC cells proliferation. (E) Colony formation assay showing the proliferation of the SNX5 overexpressed cells. (F) Colony

formation assay showing the proliferation of the SNX5 knockdown cells. (G) In vivo growth assays showing the difference in tumor diameter and weight between SNX5 overexpressing cells and the control group. (H) In vivo growth assays showing the difference in tumor diameter and weight between SNX5 knockdown cells and the control group. (I) IHC assay showing that the expression of Ki-67 and PCNA in overexpressing SNX5 ccRCC cells. (J) IHC assay showing that the expression of ki-67 and PCNA in knockdown SNX5 ccRCC cells. *P< 0.05; **P< 0.01

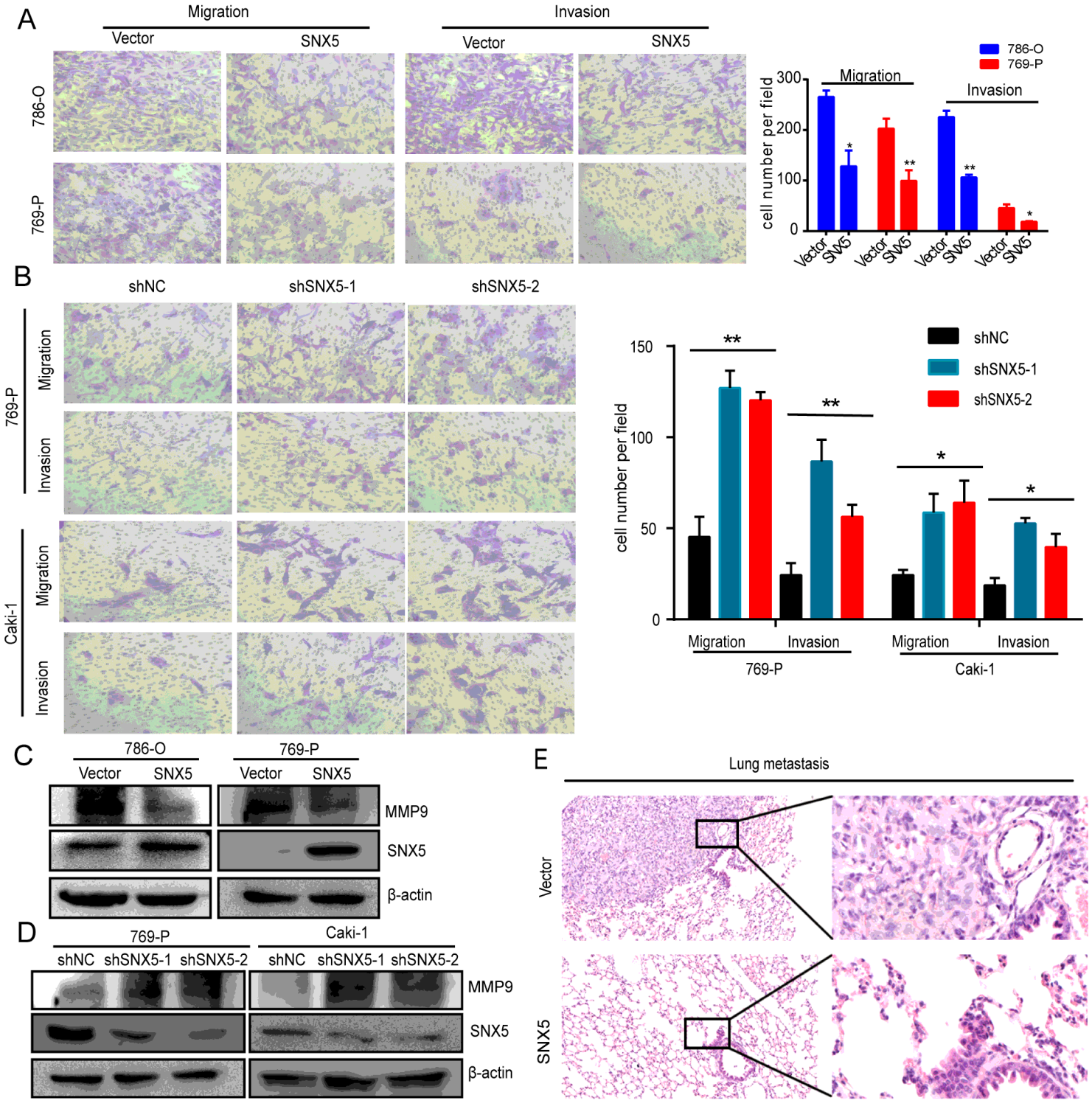

Figure 3

SNX5 inhibits ccRCC cell migration and invasion. (A) Transwell analysis showed that the overexpression of SNX5 inhibited ccRCC cells migration and invasion. (B) Transwell analysis showed that knockdown of SNX5 promoted ccRCC cells migration and invasion.(C) The expression of MMP9 was detected by Western blot in SNX5-overexpressing cells and (D)SNX5 knocked down cells.(E) H&E staining showing that lung metastasis in mice injected via tail vein.

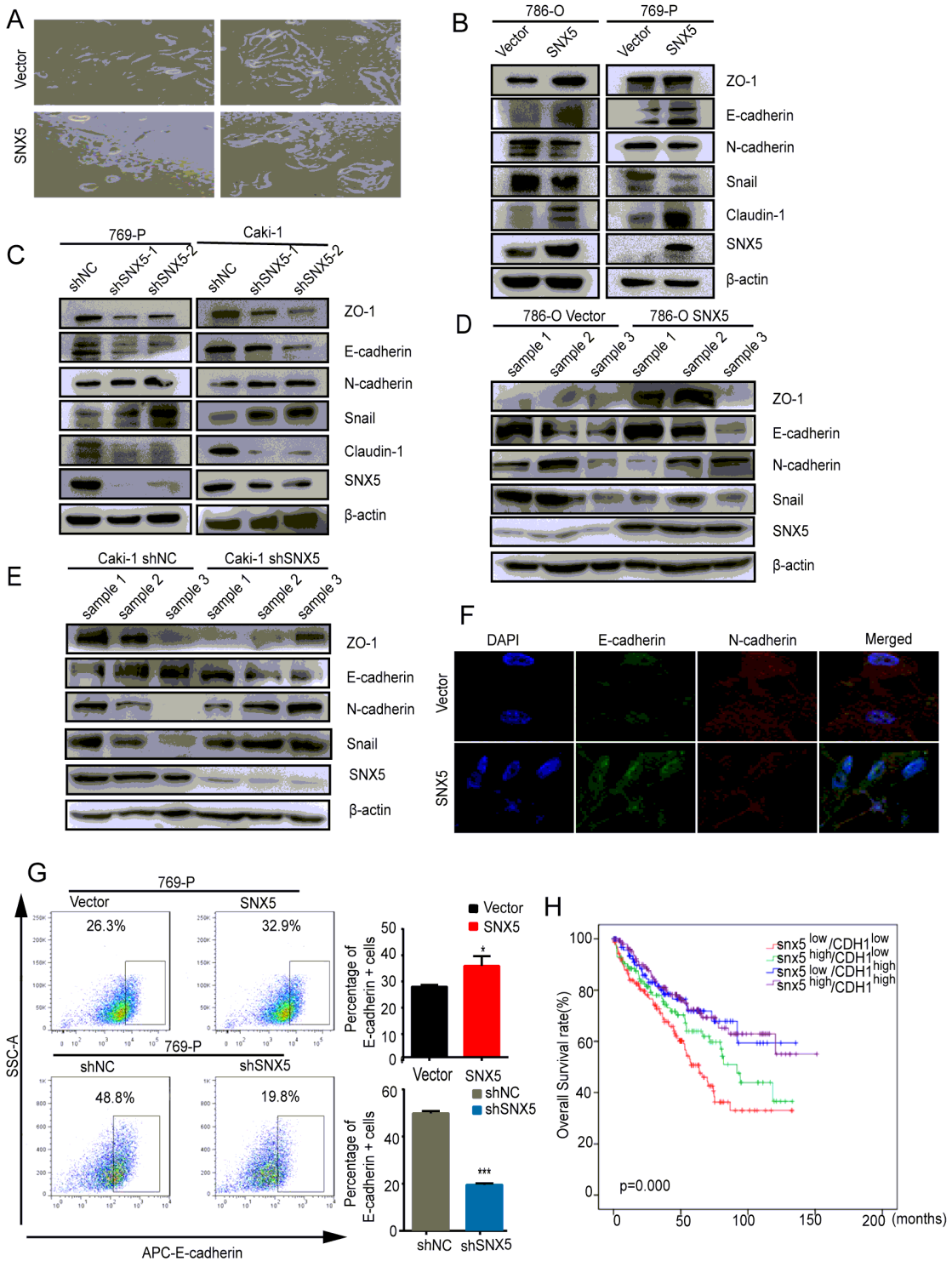

Figure 4

SNX5 suppresses epithelial-to-mesenchymal transition of ccRCC. (A) Representative images of cell morphology in SNX5-overexpressing786-O and 769-P cells. Western blot analysis of epithelial marker (E-cadherin, Zo-1Claudin-1) and mesenchymal marker (N-cadherin, snail) expression in SNX5-overexpressing cells (B) and SNX5 knockdown cells (C). Western blot analysis of epithelial marker (E-cadherin, Zo-1, Claudin-1) and mesenchymal marker (N-cadherin, snail) expression in SNX5 overexpressing tumor tissue (D) and SNX5 knockdown tumor tissue (E). (F) SNX5-overexpressing 769-P cells were applied to immunofluorescence staining. Antibodies against E-cadherin and N-cadherin were used. (G) E-cadherin on the cell surface in SNX5-overexpressing and SNX5 knockdown 769-P cells was assessed by flow cytometry. (H) Kaplan-Meier analysis of the correlation between the combined expression of SNX5 and E-cadherin with the overall survival of kidney cancer patients according to data sets from TCGA ($P<0.01$, log-rank test).

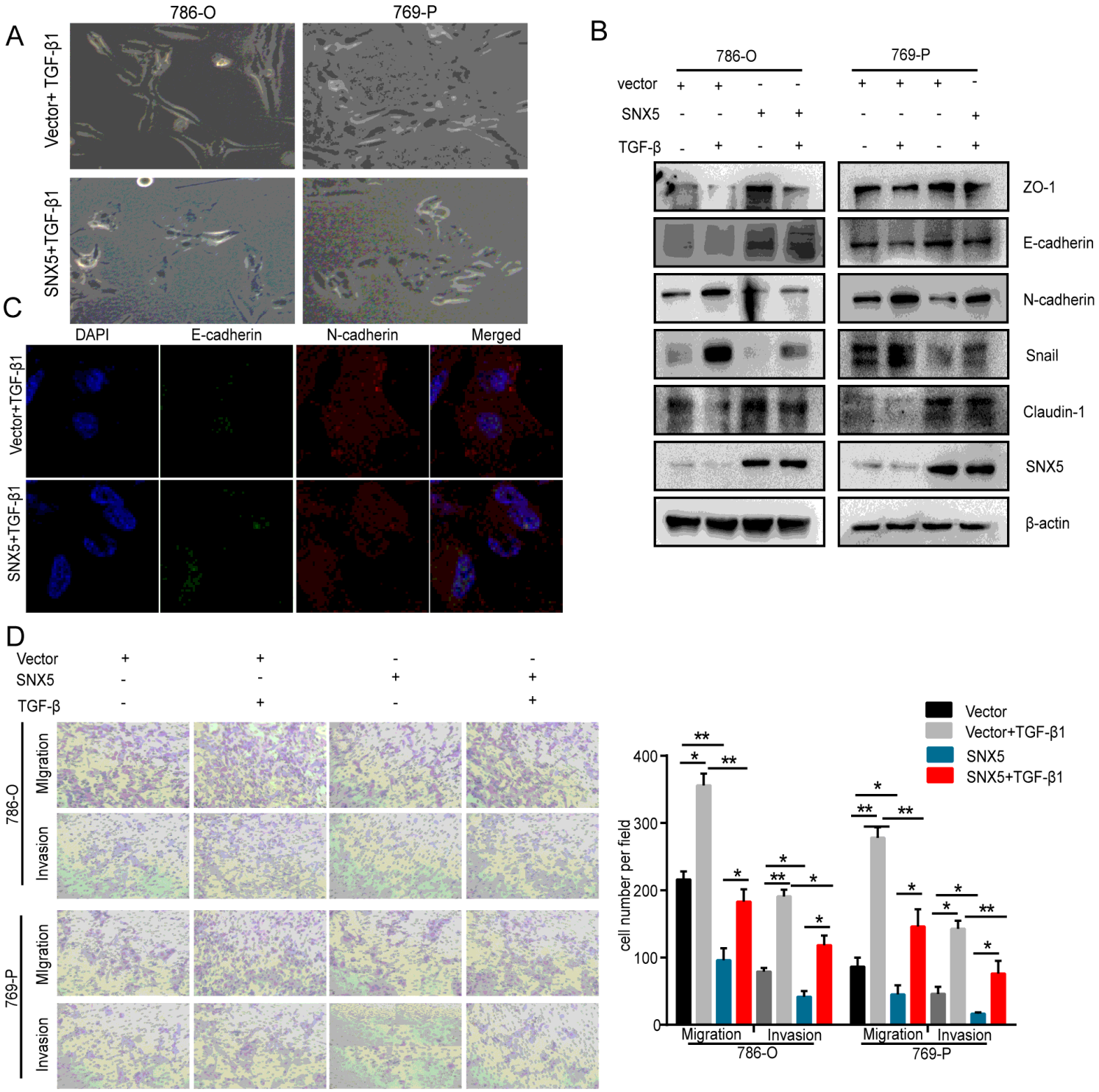

Figure 5

SNX5 inhibits EMT conversion partially reversed by TGF-β. (A) Representative images of cell morphology in SNX5-overexpressing786-O and 769-P cells with TGF-β treated. (B)Western blot analysis of epithelial marker (E-cadherin, ZO-1、Claudin-1) and mesenchymal marker (N-cadherin, snail) expression in SNX5-overexpressing786-O and 769-P cells with TGF-β treated. (C)SNX5-overexpressing 769-P cells with TGF-β treated were applied to immunofluorescence staining. Antibodies against E-cadherin and N-cadherin were

used. (D) SNX5-overexpressed ccRCC cells were treated with TGF-β or control, and cell migration and invasion were evaluated by a transwell assay.*P<0.05; **P<0.01.

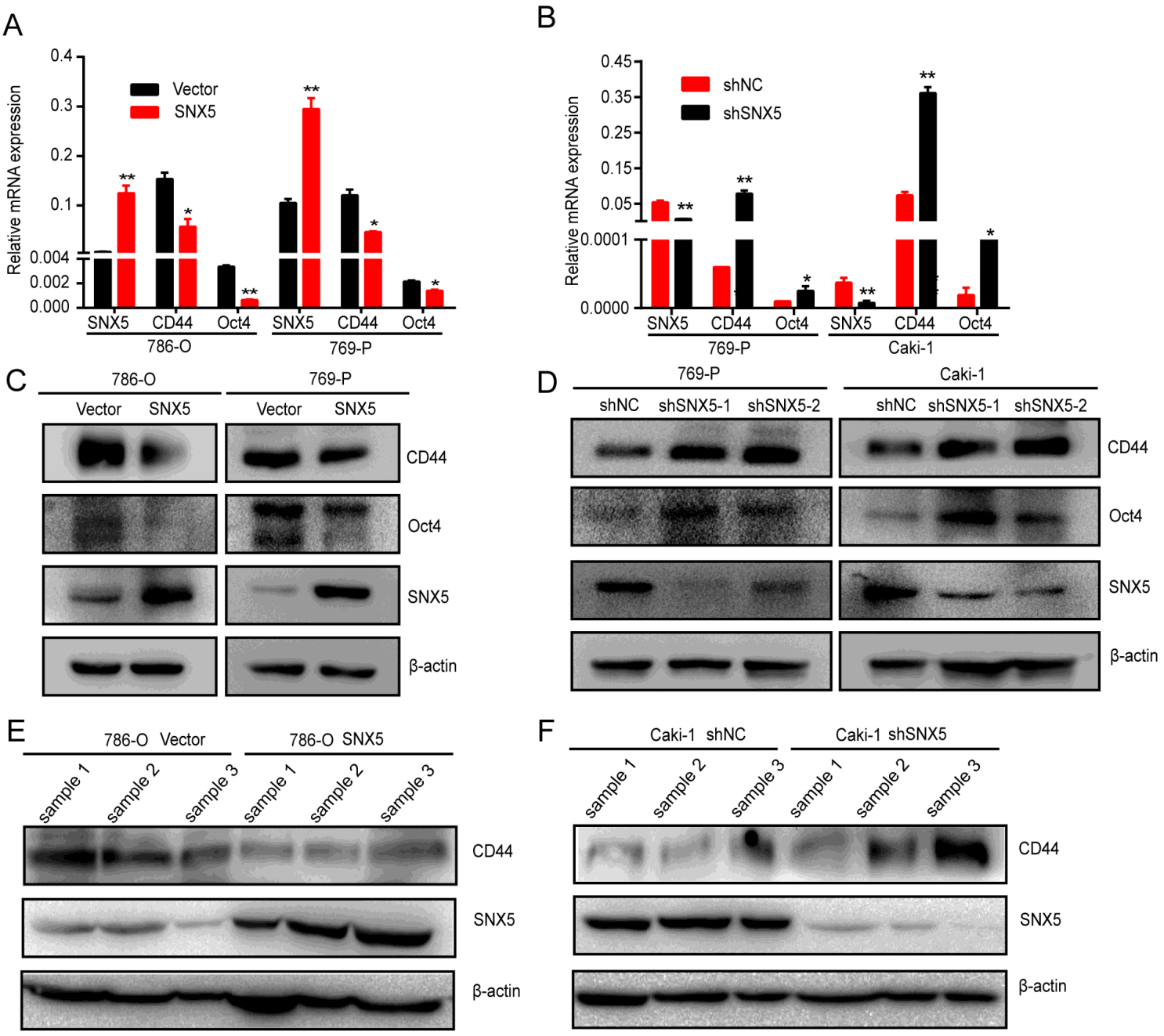

Figure 6

SNX5 inhibits ccRCC cell stemness. (A) The expression of CD44, Oct4 and SNX5 was detected by qRT-PCR in SNX5-overexpressing 786-O and 769-P cells.(B) The expression of CD44, Oct4 and SNX5 was detected byqRT-PCR in SNX5-knockdown 769-P and Caki-1 cells. Western blot analysis of CD44, Oct4 and SNX5 in SNX5-overexpressing cells (C) and SNX5 knockdown cells (D). Western blot analysis of CD44, SNX5 in SNX5-overexpressing tumor tissue (E) and SNX5 knockdown tumor tissue (F). *P< 0.05; **P< 0.01.

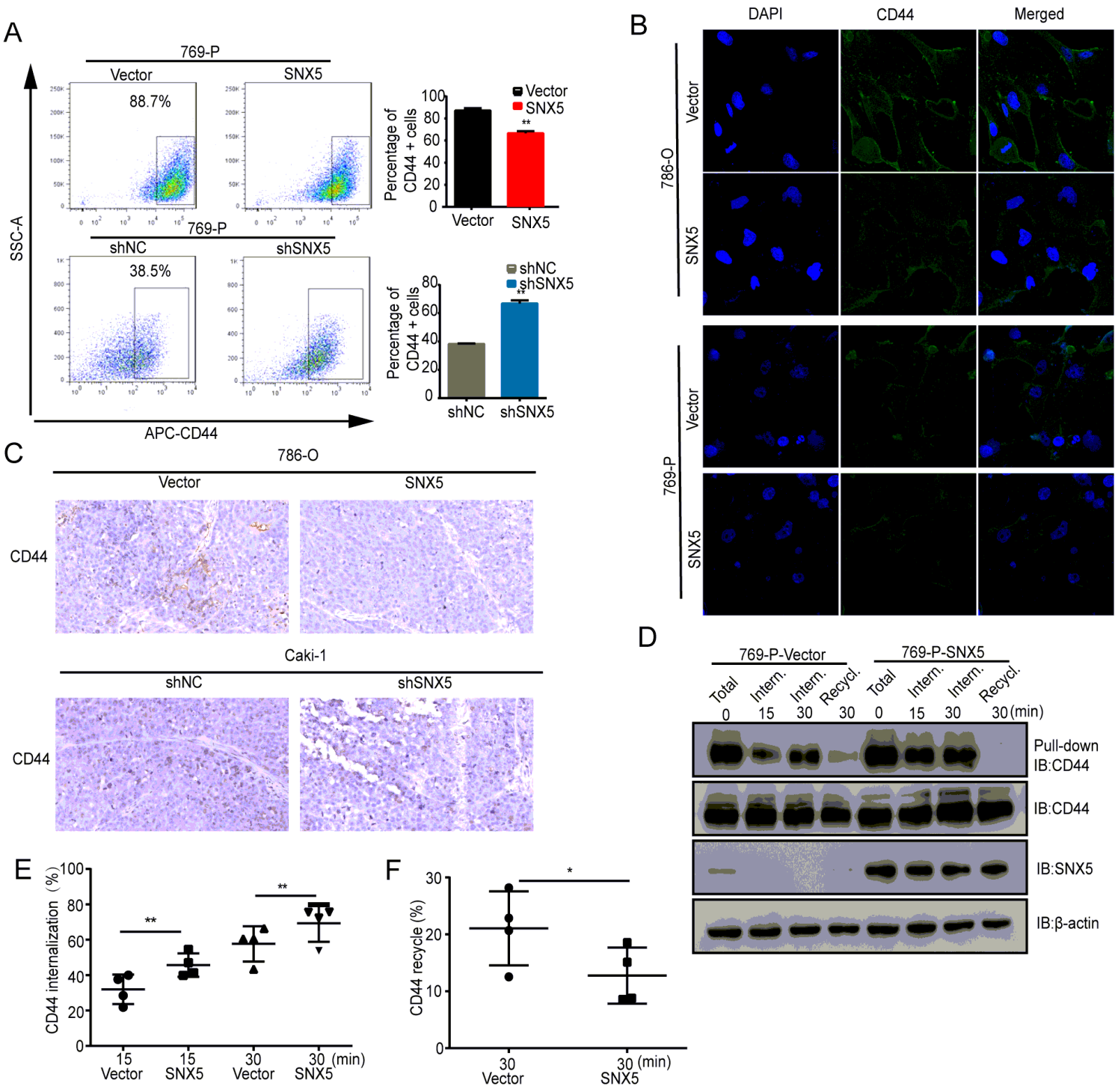

Figure 7

SNX5 influences CD44 endosomal trafficking. (A) CD44 on the cell surface in SNX5-overexpressing and SNX5 knockdown 769-P cells was assessed by flow cytometry. (B) SNX5-overexpressing 786-O and 769-P cells were applied to immunofluorescence staining. (C) IHC shows that the expression of CD44 in SNX5-overexpressing tumor tissue and knockdown SNX5 tumor tissue. (D) Cells were surface-labeled with cleavable biotin at 4 °C, left alone to allow internalization or recycling, and examined by Western blotting. (E) Quantification of internalized CD44 in SNX5 overexpressing cells from (D). (F) Quantification of recycled CD44 in SNX5 overexpressing cells from (D).*P< 0.05; **P< 0.01.

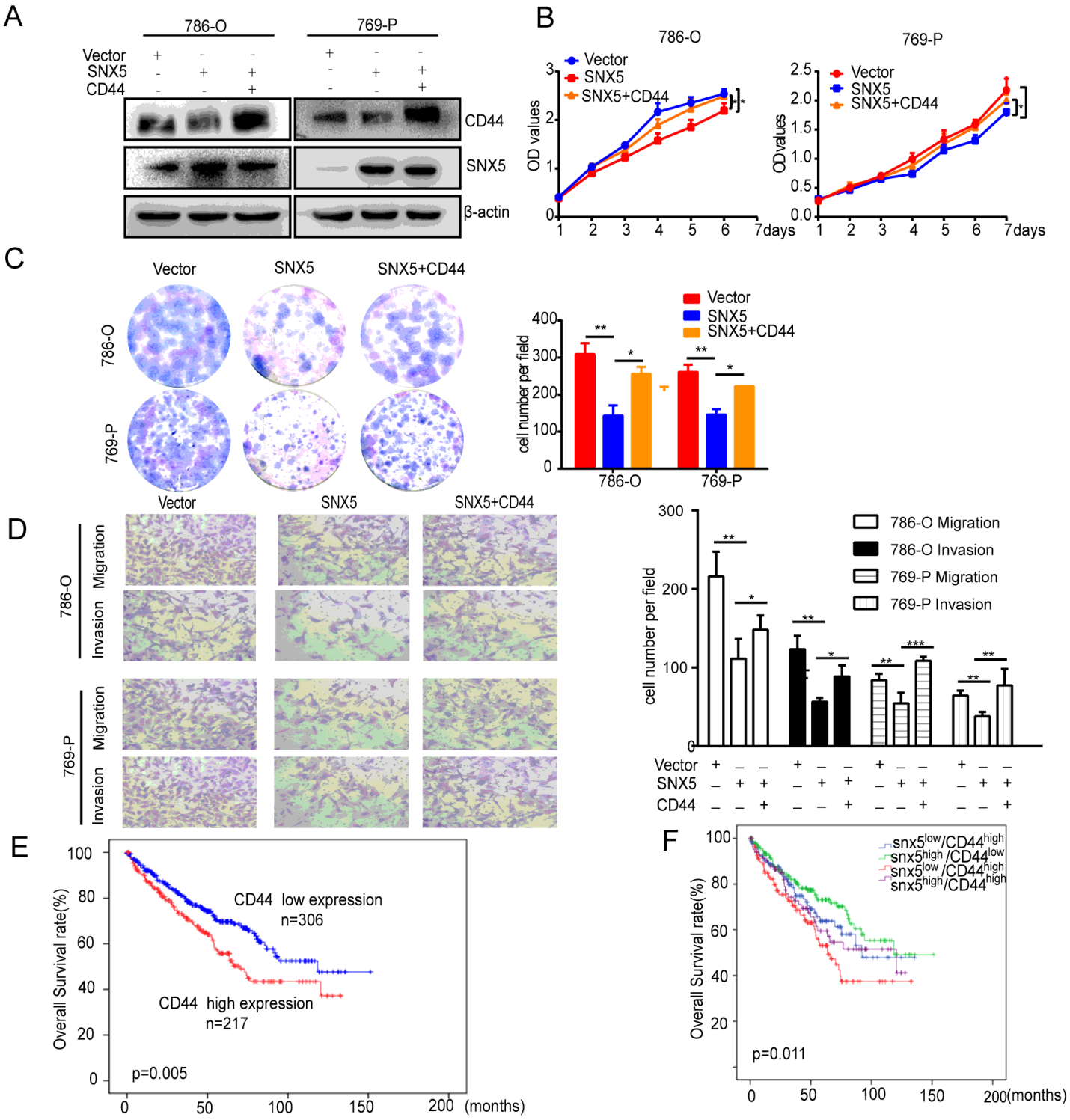

Figure 8

SNX5 suppresses ccRCC cell proliferation, migration and invasion by CD44 pathway. (A) SNX5-overexpressing 786-O and 769-P cells were overexpressed CD44 as indicated, and CD44 and SNX5 expression was detected by western blot.(B) Cell proliferation was assessed by the CCK8 assay in SNX5-overexpressing 786-O and 769-P cells overexpressed CD44.(C) Cell proliferation was assessed by colony formation assay the in SNX5-overexpressing 786-O and 769-P cells overexpressed CD44.(D) Cell

migration and invasion were assessed by the transwell assay in SNX5-overexpressing 786-O and 769-P cells overexpressed CD44. (E) Kaplan–Meier analysis of showing the overall survival of the high and low expression groups based on CD44 levels according to data sets from TCGA (P=0.005, log-rank test). (F) Kaplan-Meier analysis of the correlation between the combined expression of SNX5 and CD44 with the overall survival of kidney cancer patients according to data sets from TCGA (P=0.011, log-rank test).*P< 0.05; **P< 0.01.

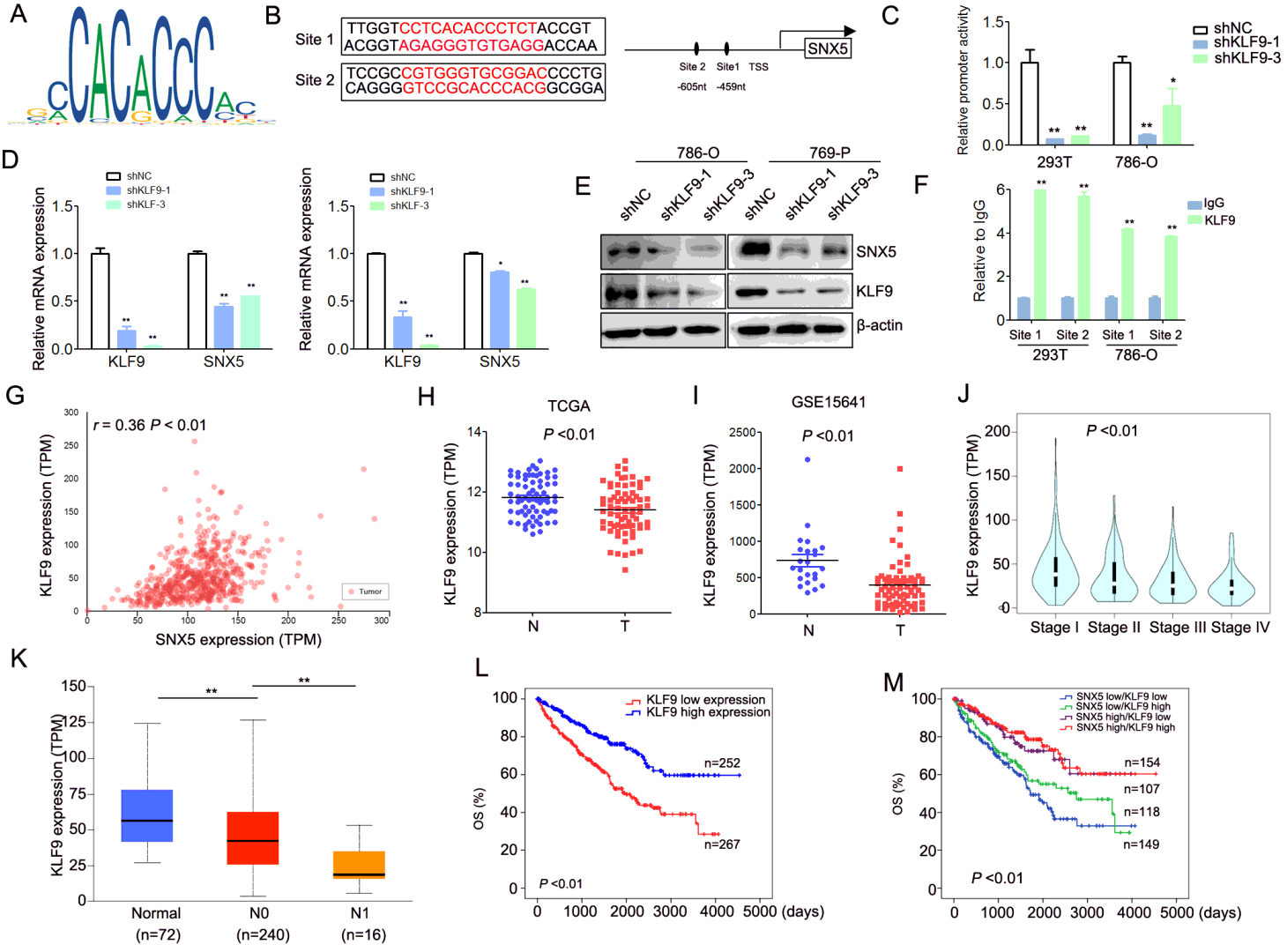

Figure 9

KLF9 binds to the SNX5 promoter and is positively correlated with SNX5 expression in ccRCC tissues and predicts a poor prognosis. (A) KLF9 binding motif. (B) KLF9 DNA-binding sites are present in the human SNX5 promoter region. (C) 786-O and HEK-293T cells were transfected with SNX5 luciferase reporter vectors and KLF9 shRNA. The corresponding luciferase activities were determined by reporter gene assays. (D) The expression of SNX5 mRNA was detected by qRT-PCR in ccRCC cells transfected with KLF9 shRNA or shNC. (E) The expression of SNX5 protein was detected by Western Blotting in ccRCC cells transfected with KLF9 shRNA or shNC.(F) qRT-PCR for ChIP analysis of KLF9 binding to the SNX5

promoter.(G) The expression of KLF9 was negative associated with tumor stage using data sets from TCGA. (H) The expression of KLF9 in ccRCC tissues compared with adjacent normal tissues was analyzed using data sets from TCGA. (I) The expression of KLF9 in ccRCC tissues compared with adjacent normal tissues was analyzed using data sets from GSE15641. (J) The correlation between KLF9 expression and tumor stage in ccRCC was analyzed using TCGA data sets. (K) The correlation between KLF9 expression and nodal metastasis status in ccRCC was analyzed using TCGA data sets. (L) OS analysis of patients with ccRCC stratified by the KLF9 expression level using TCGA data sets. (M) Kaplan-Meier analysis of the correlation between the combined expression of SNX5 and KLF9 with the overall survival of kidney cancer patients according to data sets from TCGA ($P<0.01$, log-rank test).*$P< 0.05$; **$P< 0.01$.

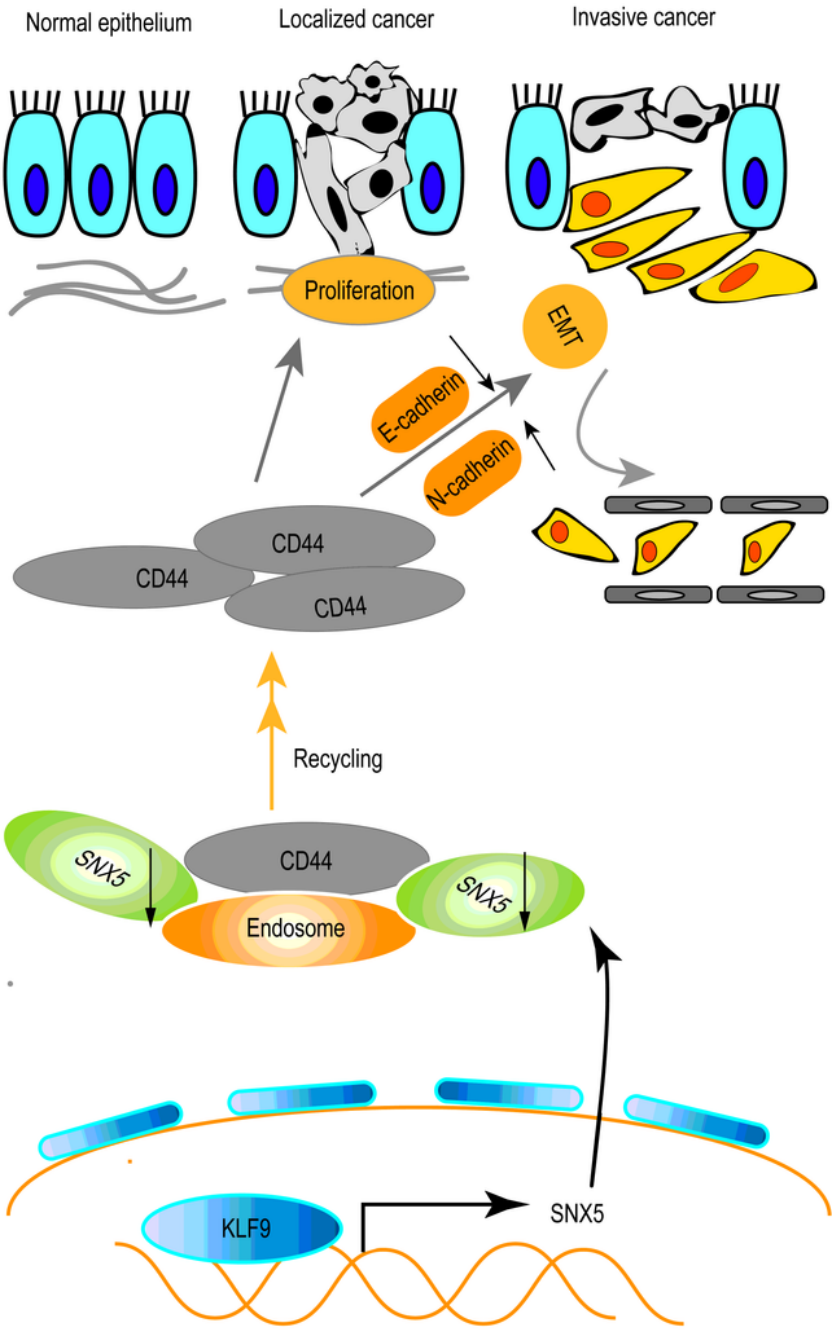

Figure 10

Representative model of this study. SNX5 is transcriptionally upregulated by KLF9 in ccRCC. KLF9 deficiency causes a decrease of SNX5 levels, with a consequent increase of CD44 trafficking and recycling, subsequently induces EMT and promotes cell proliferation, invasion and metastasis in human ccRCC.

Supplementary Files

This is a list of supplementary files associated with this preprint. Click to download.

- supplementarydata1.docx